



Tunable Curie temperature in $\text{Mn}_{1.15}\text{Fe}_{0.85}\text{P}_{0.55}\text{Si}_{0.45}$ via lattice engineering by Al addition

Sumin Kim^{a,1}, Hyunjun Shin^{a,1}, Inchang Chu^b, Kyungmi Lee^a, Kyu Hyung Lee^{a,*}, Wooyoung Lee^{a,*}

^a Department of Materials Science and Engineering, Yonsei University, Seoul 03722, South Korea

^b Research and Development Division, Hyundai Motor Company, Uiwang 16082, South Korea



ARTICLE INFO

Article history:

Received 1 April 2021

Received in revised form 18 August 2021

Accepted 29 August 2021

Available online 31 August 2021

Keywords:

$\text{Mn}_{1.15}\text{Fe}_{0.85}\text{P}_{0.55}\text{Si}_{0.45}$

Magnetocaloric material

Curie temperature

Doping

Lattice engineering

ABSTRACT

Bulk polycrystalline samples of hexagonal Fe_2P -type Al-added $\text{Mn}_{1.15}\text{Fe}_{0.85}\text{P}_{0.55}\text{Si}_{0.45}$ were prepared via a solid-state reaction under controlled heat treatment, and their magnetocaloric properties, including magnetization and entropy change, were investigated. Notably, the Curie temperature, which is directly related to the operating temperature of magnetocaloric materials, could be systematically tuned through Al substitution at Si sites owing to the lattice engineering effect. We found an inverse relationship between the Curie temperature and the ratio of the c -axis lattice constant to a -axis lattice constant, which enables the design of magnetocaloric materials for high-performance magnetic cooling systems.

© 2021 Elsevier B.V. All rights reserved.

1. Introduction

The existing cooling method based on vapor compression has certain disadvantages, such as low efficiency, a large volume, and the emission of environmentally harmful gases. In contrast, magnetic refrigeration based on the magnetocaloric effect not only provides high cooling efficiency but also offers several advantages, such as high stability, low noise, and eco-friendliness [1–5]. Thus, magnetic refrigeration is emerging as an alternative technology that can replace vapor-compression refrigeration. The magnetic refrigeration technology relies on the magnetocaloric effect, a phenomenon whereby the temperature of a material is changed by modulating the magnitude of an external magnetic field. Magnetic cooling is used in temperature-control systems, especially for low temperature ranges; however, cost-effective, high-performance magnetocaloric materials are required for wider application of magnetic cooling.

Gd-, La-, Fe_2P -, and MnNi-based materials have been studied extensively owing to their excellent magnetocaloric properties near room temperature [6–8]. Among them, Gd-based alloys offer many

advantages, such as a wide driving range and low hysteresis; however, they require a high magnetic field for the operation of the cooling system, which is a critical problem alongside the elevated material cost of Gd, a rare-earth element [9–12]. Hitherto, Fe_2P -type MnFeP-based compounds have been considered as promising candidates owing to their low material cost, non-toxicity, and large magnetocaloric effect [13–21]. However, certain challenges, such as controlling the magnetic transition temperature arising from the intrinsic first-order magnetic transition [22–27] and enhancing the magnetic cooling performance, remain to be overcome.

Lattice engineering via compositional tuning is a simple and highly reproducible approach for inducing a change in the magnetic properties of a magnetic material, because the electronic and spin structures are largely dependent on the crystal structure. For example, in the case of the MnFeP-based system [28,29], the magnetic transition temperature can be tuned by doping another element at the P site owing to the lattice distortion caused by an external magnetic field. Herein, we present experimental findings regarding the tunable magnetic properties of $\text{Mn}_{1.15}\text{Fe}_{0.85}\text{P}_{0.55}\text{Si}_{0.45}$ achieved via lattice engineering through Al substitution at the Si site. The Curie temperature (T_C) of this material could be systematically tuned by controlling the ratio of the c -axis lattice constant (c) to the a -axis lattice constant (a), i.e., the c/a ratio.

* Corresponding authors.

E-mail addresses: khlee2018@yonsei.ac.kr (K.H. Lee), wooyoung@yonsei.ac.kr (W. Lee).

¹ These authors contributed equally.

2. Experimental section

Ingots of $\text{Mn}_{1.15}\text{Fe}_{0.85}\text{P}_{0.55}\text{Si}_{0.45-x}\text{Al}_x$ ($0 \leq x \leq 0.025$) were prepared through an arc melting process using a mixture of the precursors (high purity (>99.9%) Mn, Fe, FeP, Si, and Al) in an Ar atmosphere. Powder precursors (<53 μm) of the ingots were obtained via ball milling and sieving, and the cold-pressed disc-type samples were then loaded into a vacuum-sealed quartz tube ($\sim 10^{-3}$ Torr) to prevent oxidation. Finally, bulk samples were obtained through sintering at temperatures of 1323–1423 K for 50 h.

To investigate the phase formation behavior of the sintered $\text{Mn}_{1.15}\text{Fe}_{0.85}\text{P}_{0.55}\text{Si}_{0.45-x}\text{Al}_x$ ingots, we performed X-ray diffraction (XRD, Ultima IV, Rigaku Corp., Japan) with $\text{Cu-K}\alpha_1$ radiation ($\lambda = 1.54059 \text{ \AA}$). The dependences of the DC magnetization (M) on the temperature (T) and magnetic field (H) were evaluated with a vibrating sample magnetometer in the range of $T = 200\text{--}400 \text{ K}$ and $H = -1$ to 1 T , using a physical property measurement system (Quantum Design, Inc., USA).

3. Results and discussion

First, we optimized the heat-treatment condition to obtain single-phase materials because of the compositional complexity of the MnFeP-based compounds [18,19]. Fig. 1 shows the XRD patterns of the sintered pristine $\text{Mn}_{1.15}\text{Fe}_{0.85}\text{P}_{0.55}\text{Si}_{0.45}$ samples. The XRD peaks could be matched well with those of Fe_2P or Mn_2P with a hexagonal structure (space group, $P\text{-}62m$). However, peaks of secondary phases were also clearly observed for all the samples, except for the sample sintered at 1373 K. This indicates that the heat-treatment window for generating a single phase is very narrow. It was confirmed that a small amount of Fe_2MnSi was formed in the

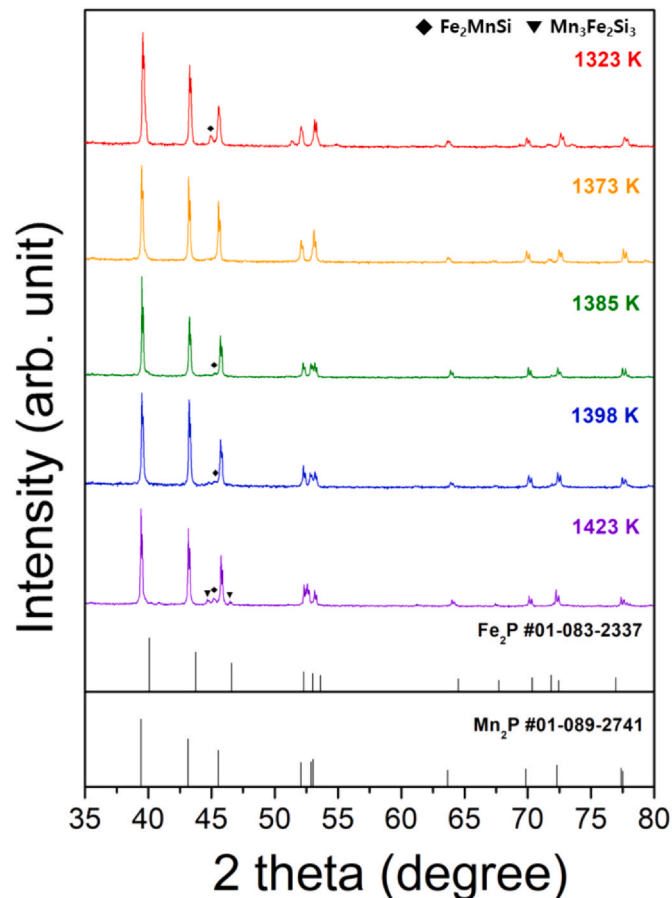


Fig. 1. XRD patterns of the bulk polycrystalline samples of $\text{Mn}_{1.15}\text{Fe}_{0.85}\text{P}_{0.55}\text{Si}_{0.45}$.

samples heat-treated at 1323, 1385, and 1398 K, whereas both Fe_2MnSi and $\text{Mn}_3\text{Fe}_2\text{Si}_3$ were produced in the sample heat-treated at 1423 K. Thus, the heat-treatment temperature for Al-added $\text{Mn}_{1.15}\text{Fe}_{0.85}\text{P}_{0.55}\text{Si}_{0.45}$ was set at 1373 K.

To investigate the magnetic properties of pristine $\text{Mn}_{1.15}\text{Fe}_{0.85}\text{P}_{0.55}\text{Si}_{0.45}$ sintered at 1373 K, the temperature-dependent magnetization (M) was assessed at $H = 1 \text{ T}$ upon warming after zero-field cooling (ZFC) under the same field. Using the recorded heating curve, the characteristic of the first-order magnetic transition was confirmed, as shown in Fig. 2(a), and T_C was observed to be $\sim 284 \text{ K}$. In general, the T_C of $(\text{Mn,Fe})_2(\text{P,Si})$ -based compounds can be controlled by varying the P/Si ratio or Mn/Fe ratio [14,30]. We differentiated the M - T curve with respect to temperature and calculated the entropy change based on the fundamental thermodynamic relationship given in Eq. (1):

$$S(T, H) = -\frac{\partial F(T, H)}{\partial T} \quad (1)$$

where $S(T, H)$ is the entropy function, and F is the Helmholtz free energy. As shown in Fig. 2(b), the maximum entropy change ($-\Delta S_M$), i.e., $14.57 \text{ J kg}^{-1} \text{ K}^{-1}$, occurred at $T = 279 \text{ K}$.

The curves for the initial isothermal magnetization (M_{iso}) of $\text{Mn}_{1.15}\text{Fe}_{0.85}\text{P}_{0.55}\text{Si}_{0.45}$ were also obtained in the temperature range of 200–280 K (in steps of 10 K between 200 and 260 K and in steps of 4 K between 260 and 280 K) (Fig. 3(a)). As the temperature increased, the maximum magnetization at $H = 1 \text{ T}$ gradually decreased, and the magnetization subsequently tended to decrease rapidly near the magnetic transition temperature. In particular, the shape of the initial M - H curve changed rapidly because the ferromagnetic ordering disappeared due to the change in the magnetic structure with increasing temperature. Fig. 3(b) presents the change in the magnetic entropy calculated using the initial M - H curve, based on the Maxwell relation (Eq. (2)):

$$\Delta S_M(T, H) = -\mu_0 \int_0^{H_f} \frac{\partial M(T, H)}{\partial T} dH \quad (2)$$

where μ_0 is the magnetic permeability in vacuum, H_f is the end point of H for the integral ($H_f = 1 \text{ T}$), and $\frac{\partial M(T, H)}{\partial T}$ is the T gradient of M . The approximate $\frac{\partial M(T, H)}{\partial T}$ value was calculated from the slope of two adjacent data points. A $-\Delta S_M$ value of $14.4 \text{ J kg}^{-1} \text{ K}^{-1}$ was obtained at $T = 268 \text{ K}$. A difference of $\sim 11 \text{ K}$ was observed between the peak temperature values corresponding to the M - T and M - H curves. This is attributed to the difference in the measurement method; the M - T curve was obtained under a varying temperature change, while the M - H curve was obtained under a static temperature. In addition, it was confirmed that the magnetic entropy change values calculated from the M - H and M - T curves did not differ significantly.

Fig. 4(a) shows the temperature-dependent magnetization of the $\text{Mn}_{1.15}\text{Fe}_{0.85}\text{P}_{0.55}\text{Si}_{0.45-x}\text{Al}_x$ ($x = 0.005\text{--}0.025$) alloys under an external magnetic field of $H = 1 \text{ T}$. After the first-order transition, the net magnetization of all the samples converged to almost zero at high temperatures. However, the Al-added samples exhibited lower saturation magnetization values than the pristine $\text{Mn}_{1.15}\text{Fe}_{0.85}\text{P}_{0.55}\text{Si}_{0.45}$ sample did. This is related to the change in the magnetic structure owing to the substitution of Al at the Si sites in the lattice. Fig. 4(b) shows the magnetic entropy change calculated using the M - T curve based on the fundamental thermodynamic relationship. The entropy change values of Al-added samples were smaller than that of the pristine $\text{Mn}_{1.15}\text{Fe}_{0.85}\text{P}_{0.55}\text{Si}_{0.45}$ sample; this was because of the formation of the secondary phase of $\text{Mn}_3\text{Fe}_2\text{Si}_3$ owing to the solubility limit of Al at the Si site, as shown in Fig. 5(a) [15]. It was also confirmed by SEM(scanning electron microscopy)-EDS(energy dispersive spectroscopy) that Al was substituted (Figs. S3 and S4). As shown in Fig. S4, it was verified that Al was evenly distributed suggesting substitution at Si-site. However, the variation in T_C observed in Fig. 4

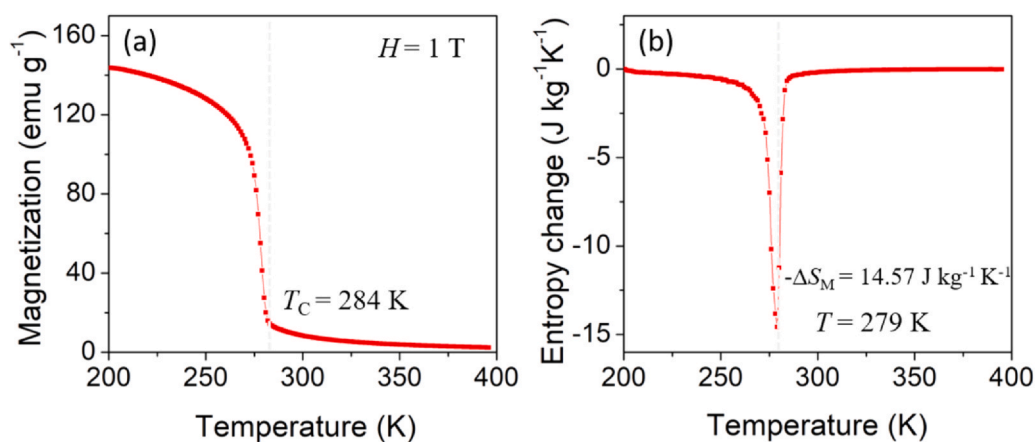


Fig. 2. (a) Magnetization as a function of temperature for $\text{Mn}_{1.15}\text{Fe}_{0.85}\text{P}_{0.55}\text{Si}_{0.45}$ under an external magnetic field, $H = 1$ T. (b) Entropy change of $\text{Mn}_{1.15}\text{Fe}_{0.85}\text{P}_{0.55}\text{Si}_{0.45}$ for a magnetic field change of $\Delta H = 1$ T, calculated using the fundamental thermodynamic relation.

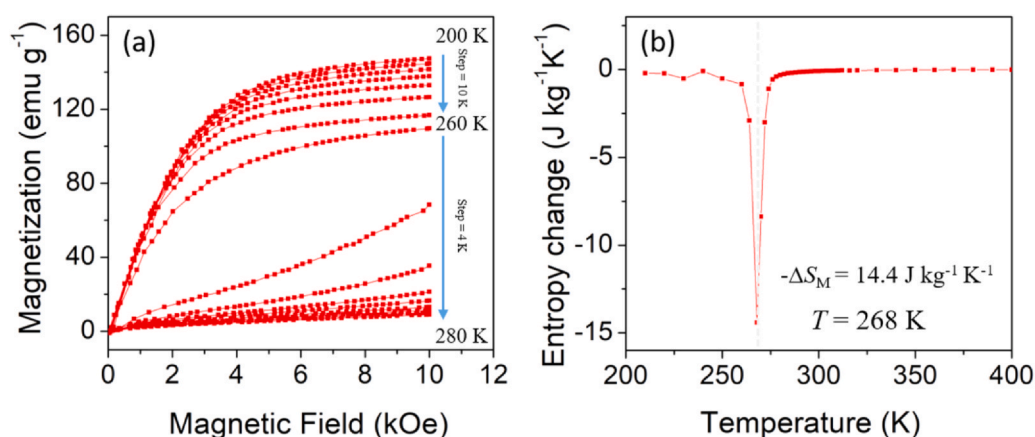


Fig. 3. (a) Initial isothermal magnetization curves for $\text{Mn}_{1.15}\text{Fe}_{0.85}\text{P}_{0.55}\text{Si}_{0.45}$. (b) Entropy change of $\text{Mn}_{1.15}\text{Fe}_{0.85}\text{P}_{0.55}\text{Si}_{0.45}$ for a magnetic field change of $\Delta H = 1$ T, calculated using the Maxwell relation.

is an unusual feature, despite the formation of a secondary phase. To elucidate this, we calculated T_C according to the Al content; and the values are plotted in Fig. 5(b). T_C increases with the Al content and reaches a maximum value of 317 K for $\text{Mn}_{1.15}\text{Fe}_{0.85}\text{P}_{0.55}\text{Si}_{0.44}\text{Al}_{0.01}$; thereafter, it decreases with a further increase in the Al content. This result is considered to be related to the structural change due to Al substitution at the Si site in the lattice. Therefore, we calculated the

lattice constant a and c via Rietveld refinement of the XRD patterns; the extracted parameters are shown in Fig. 5(c). From the relationships between T_C and several structural parameters, we found an inverse dependence of T_C on c/a , which suggests that T_C can be engineered using a simple compositional tuning approach based on Al substitution. Chemical pressure is known to be one of the causes of changes in T_C [31,32]. Thus, the increased T_C could be attributed to the

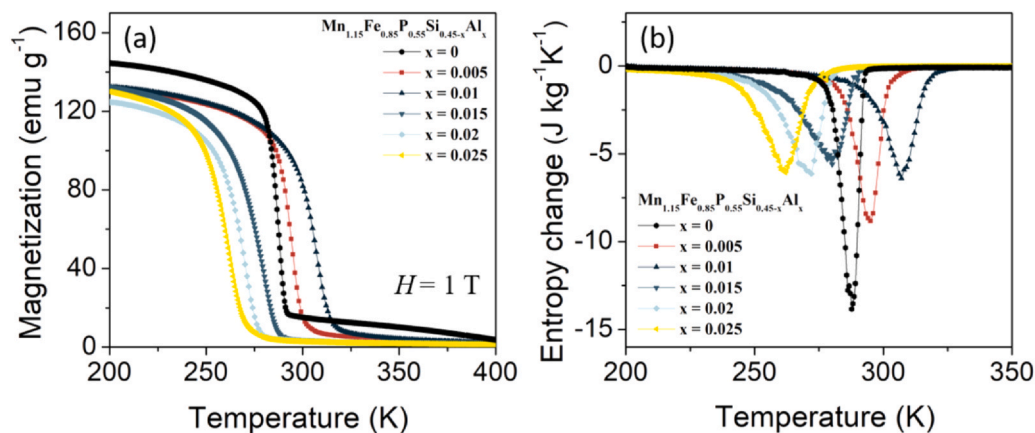


Fig. 4. (a) Magnetization as a function of temperature for $\text{Mn}_{1.15}\text{Fe}_{0.85}\text{P}_{0.55}\text{Si}_{0.45-x}\text{Al}_x$ ($x = 0-0.025$) under an external magnetic field, $H = 1$ T. (b) Entropy change of $\text{Mn}_{1.15}\text{Fe}_{0.85}\text{P}_{0.55}\text{Si}_{0.45-x}\text{Al}_x$ ($x = 0-0.025$) for a magnetic field change of $\Delta H = 1$ T, calculated using the fundamental thermodynamic relation.

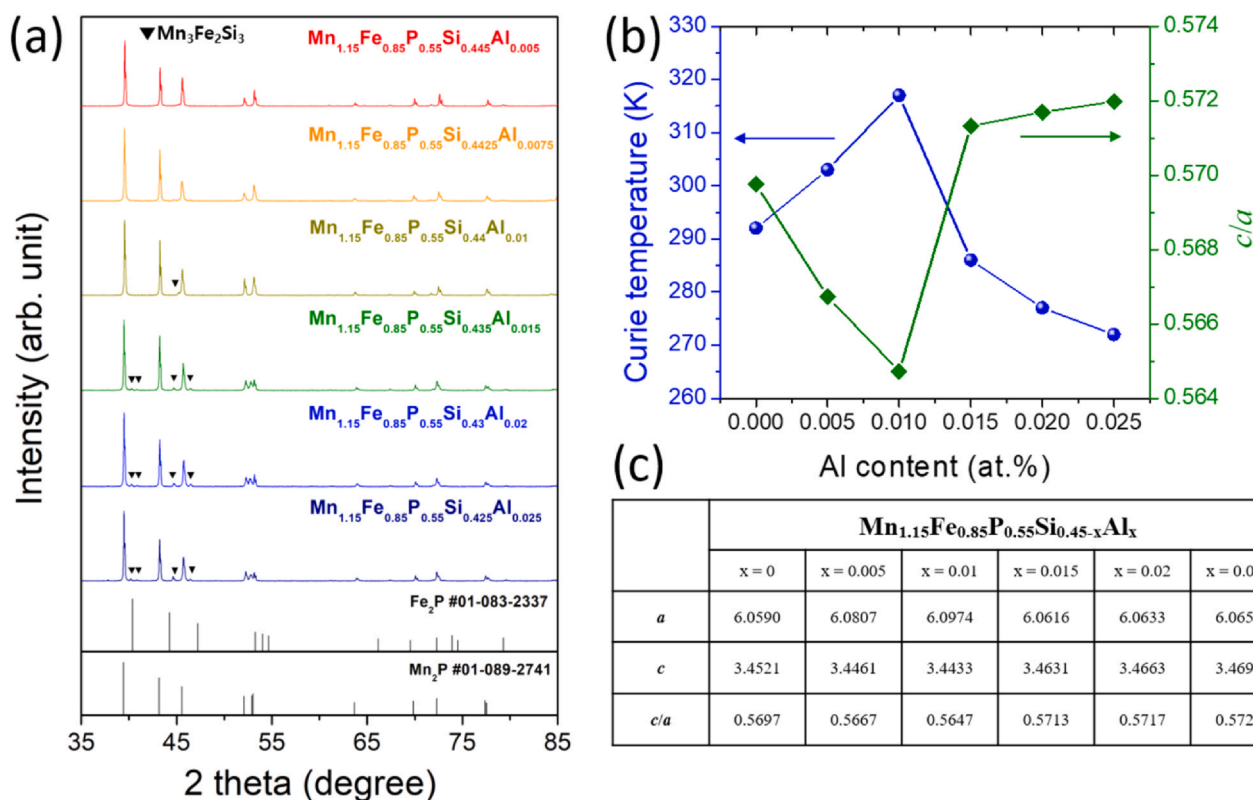


Fig. 5. (a) XRD patterns of the bulk polycrystalline samples of $\text{Mn}_{1.15}\text{Fe}_{0.85}\text{P}_{0.55}\text{Si}_{0.45-x}\text{Al}_x$ ($x = 0-0.025$). (b) Curie temperature and the lattice constant ratio (c/a) according to the Al content in $\text{Mn}_{1.15}\text{Fe}_{0.85}\text{P}_{0.55}\text{Si}_{0.45-x}\text{Al}_x$ ($x = 0-0.025$). (c) Lattice parameters of polycrystalline $\text{Mn}_{1.15}\text{Fe}_{0.85}\text{P}_{0.55}\text{Si}_{0.45-x}\text{Al}_x$ ($x = 0-0.025$) at room temperature; it crystallized with a hexagonal $P-62m$ structure.

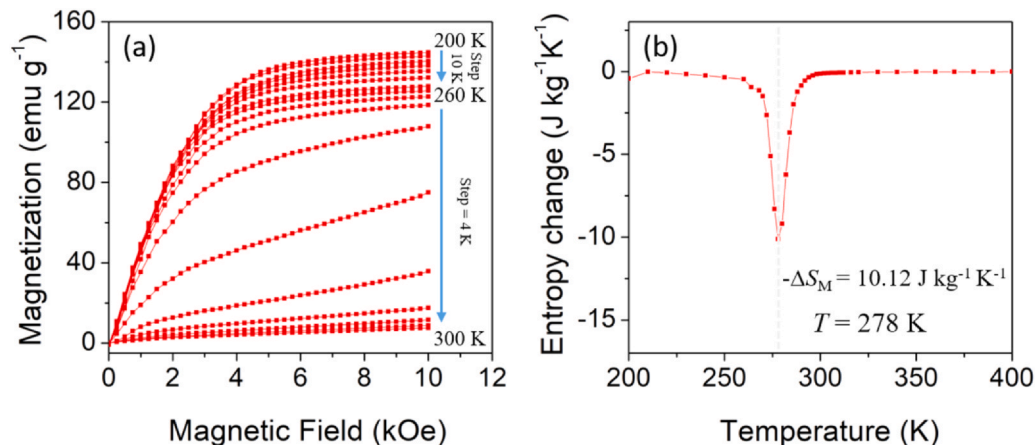


Fig. 6. (a) Initial isothermal magnetization curves of $\text{Mn}_{1.15}\text{Fe}_{0.85}\text{P}_{0.55}\text{Si}_{0.445}\text{Al}_{0.005}$. (b) Entropy change of $\text{Mn}_{1.15}\text{Fe}_{0.85}\text{P}_{0.55}\text{Si}_{0.445}\text{Al}_{0.005}$ for a magnetic field change of $\Delta H = 1$ T, calculated using the Maxwell relation.

decrease in c/a with the substitution of Al (atomic radius = 184 pm) at the Si (atomic radius = 210 pm) sites.

For the $\text{Mn}_{1.15}\text{Fe}_{0.85}\text{P}_{0.55}\text{Si}_{0.45}\text{Al}_{0.005}$ alloy, we evaluated the magnetic-field dependence of magnetization (M) by varying the magnetic field up to $H = 1$ T near T_C at temperature intervals of 2 K (Fig. 6(a)). The saturation magnetization at $H = 1$ T decreased compared with that of the pristine compound and was diminished due to thermal fluctuations with increasing temperature. Subsequently, a ferromagnetic to paramagnetic phase transition occurred near the critical temperature, resulting in a sharp decrease in magnetization. Fig. 6(b) presents the magnetic entropy change calculated from the isothermal magnetization results using the Maxwell relation. The $-\Delta S_M$ value of the Al-added sample ($\sim 10.12 \text{ kg}^{-1} \text{K}^{-1}$) was lower than

that of the pristine compound ($-\Delta S_M \sim 14.4 \text{ J kg}^{-1} \text{K}^{-1}$), mainly due to the formation of the secondary phase; moreover, the peak temperature shifted to a high value. These results suggest that the performance of magnetic cooling systems can be improved while maintaining a high entropy change if lattice-controlled materials are implemented.

4. Conclusions

We investigated the magnetocaloric properties of bulk samples of hexagonal Fe_2P -type $\text{Mn}_{1.15}\text{Fe}_{0.85}\text{P}_{0.55}\text{Si}_{0.45}$ and Al-added compounds. A single-phase pristine sample was successfully obtained via melt solidification and subsequent pressure-less sintering at a

controlled temperature; however, a small amount of the secondary phase of $\text{Mn}_3\text{Fe}_2\text{Si}_3$ was formed in the Al-added compounds owing to the low solubility limit of Al at the Si site. The pristine sample exhibited a maximum entropy change of $14.57 \text{ J kg}^{-1} \text{ K}^{-1}$ at $T = 279 \text{ K}$ and a Curie temperature of $\sim 284 \text{ K}$. Although the maximum entropy change decreased after Al addition, the ratio of the c -axis lattice constant to the a -axis lattice constant, i.e., c/a , was found to be an important material parameter that controls the Curie temperature.

CRedit authorship contribution statement

Sumin Kim: Conceptualization, Investigation, Formal analysis, Validation, Writing – original draft. **Hyunjun Shin:** Investigation, Formal analysis, Validation, Writing – original draft. **Inchang Chu:** Investigation, Validation. **Kyungmi Lee:** Investigation, Validation. **Kyu Hyoung Lee:** Supervision. **Wooyoung Lee:** Supervision.

Declaration of Competing Interest

The authors declare that they have no known competing financial interests or personal relationships that could have appeared to influence the work reported in this paper.

Acknowledgements

This research was supported by the Technology Innovation Program ('20013621', Center for Super Critical Material Industrial Technology) funded By the Ministry of Trade, Industry & Energy (MOTIE, Korea) and Basic Science Research Program through the National Research Foundation of Korea (NRF) funded by the Ministry of Education (NRF-2019R1A6A1A11055660) and Hyundai Motor Group (2019-11-1024).

Appendix A. Supplementary material

Supplementary data associated with this article can be found in the online version at [doi:10.1016/j.jallcom.2021.161798](https://doi.org/10.1016/j.jallcom.2021.161798).

References

- [1] O. Tegus, E. Brück, K.H.J. Buschow, F.R. de Boer, Transition-metal-based magnetic refrigerants for room-temperature applications, *Nature* 415 (2002) 150–152.
- [2] V.K. Pecharsky, K.A. Gschneidner Jr., Magnetocaloric effect and magnetic refrigeration, *J. Magn. Magn. Mater.* 200 (1999) 44–56.
- [3] K.A. Gschneidner Jr., V.K. Pecharsky, A.O. Tsokol, Recent developments in magnetocaloric materials, *Rep. Prog. Phys.* 68 (2005) 1479–1539.
- [4] B.F. Yu, Q. Gao, B. Zhang, X.Z. Meng, Z. Chen, Review on research of room temperature magnetic refrigeration, *Int. J. Refrig.* 26 (2003) 622–636.
- [5] V.K. Pecharsky, K.A. Gschneidner, A.O. Pecharsky, A.M. Tishin, Thermodynamics of the magnetocaloric effect, *Phys. Rev. B* 64 (2001) 144406.
- [6] T. Krenke, E. Duman, M. Acet, E.F. Wassermann, X. Moya, L. Mañosa, A. Planes, Inverse magnetocaloric effect in ferromagnetic Ni–Mn–Sn alloys, *Nat. Mater.* 4 (2005) 450–454.
- [7] J.-P. Camarillo-García, F. Hernández-Navarro, D.E. Soto-Parra, D. Ríos-Jara, H. Flores-Zúñiga, High sensitivity on caloric effects induced by stress or magnetic field in a polycrystalline Ni–Mn–In–Co–Cu shape-memory alloy, *Scr. Mater.* 166 (2019) 92–95.
- [8] Y. Zhang, Q. Zheng, W. Xia, J. Zhang, J. Du, A. Yan, Enhanced large magnetic entropy change and adiabatic temperature change of $\text{Ni}_{43}\text{Mn}_{46}\text{Sn}_{11}$ alloys by a rapid solidification method, *Scr. Mater.* 104 (2015) 41–44.
- [9] V.K. Pecharsky, J.K.A. Gschneidner, Giant magnetocaloric effect in $\text{Gd}_5(\text{Si}_2\text{Ge}_2)$, *Phys. Rev. Lett.* 78 (1997) 4494–4497.
- [10] J. Du, Q. Zheng, Y.B. Li, Q. Zhang, D. Li, Z.D. Zhang, Large magnetocaloric effect and enhanced magnetic refrigeration in ternary Gd-based bulk metallic glasses, *J. Appl. Phys.* 103 (2008) 023918.
- [11] Q. Luo, D.Q. Zhao, M.X. Pan, W.H. Wang, Magnetocaloric effect in Gd-based bulk metallic glasses, *Appl. Phys. Lett.* 89 (2006) 081914.
- [12] J.Y. Law, R.V. Ramanujan, V. Franco, Tunable Curie temperatures in Gd alloyed Fe–B–Cr magnetocaloric materials, *J. Alloy. Compd.* 508 (2010) 14–19.
- [13] G.F. Wang, B.Y. Yang, T. Jing, Z.R. Zhao, X.F. Zhang, Y.L. Liu, A comparative study of the magnetocaloric effect in $\text{MnFeP}_2\text{Si}_2\text{Ge}_2$ prepared by traditional sintering and spark plasma sintering, *IEEE Trans. Magn.* 55 (2019) 1–5.
- [14] B. Wurentuya, H. Yibole, F. Guillou, Z. Ou, Z. Zhang, O. Tegus, First-order magnetic transition, magnetocaloric effect and moment formation in $\text{MnFe}(\text{P},\text{Ge})$ magnetocaloric materials revisited by x-ray magnetic circular dichroism, *Phys. B: Condens. Matter* 544 (2018) 66–72.
- [15] J.W. Lai, Z.G. Zheng, B.W. Huang, H.Y. Yu, Z.G. Qiu, Y.L. Mao, S. Zhang, F.M. Xiao, D.C. Zeng, K. Goubitz, E. Brück, Microstructure formation and magnetocaloric effect of the Fe_2P -type phase in $(\text{Mn},\text{Fe})_2(\text{P},\text{Si})$ alloys, *J. Alloy. Compd.* 735 (2018) 2567–2573.
- [16] Z.Q. Ou, N.H. Dung, L. Zhang, L. Caron, E. Torun, N.H. van Dijk, O. Tegus, E. Brück, Transition metal substitution in Fe_2P -based $\text{MnFe}_{0.95}\text{P}_{0.50}\text{Si}_{0.50}$ magnetocaloric compounds, *J. Alloy. Compd.* 730 (2018) 392–398.
- [17] D. Liu, M. Yue, J. Zhang, T.M. McQueen, J.W. Lynn, X. Wang, Y. Chen, J. Li, R.J. Cava, X. Liu, Z. Altounian, Q. Huang, Origin and tuning of the magnetocaloric effect in the magnetic refrigerant $\text{Mn}_{1.1}\text{Fe}_{0.9}(\text{P}_{0.8}\text{Ge}_{0.2})$, *Phys. Rev. B* 79 (2009) 014435.
- [18] N.V. Thang, X.F. Miao, N.H. van Dijk, E. Brück, Structural and magnetocaloric properties of $(\text{Mn},\text{Fe})_2(\text{P},\text{Si})$ materials with added nitrogen, *J. Alloy. Compd.* 670 (2016) 123–127.
- [19] M. Fries, L. Pfeuffer, E. Bruder, T. Gottschall, S. Ener, L.V.B. Diop, T. Gröb, K.P. Skokov, O. Gutfleisch, Microstructural and magnetic properties of Mn–Fe–P–Si (Fe_2P -type) magnetocaloric compounds, *Acta Mater.* 132 (2017) 222–229.
- [20] Z.Q. Ou, G.F. Wang, S. Lin, O. Tegus, E. Brück, K.H.J. Buschow, Magnetic properties and magnetocaloric effects in $\text{Mn}_{1.2}\text{Fe}_{0.8}\text{P}_{1-x}\text{Ge}_x$ compounds, *J. Phys.: Condens. Matter* 18 (2006) 11577–11584.
- [21] Q. Zhou, Z.G. Zheng, W.H. Wang, L. Lei, A. He, D.C. Zeng, Carbon doping in the $\text{Mn}_{1.15}\text{Fe}_{0.80}\text{P}_{0.50}\text{Si}_{0.50}$ materials: structure, phase transition and magnetocaloric properties, *Intermetallics* 106 (2019) 94–99.
- [22] R. Fruchart, A. Roger, J.P. Senateur, Crystallographic and magnetic properties of solid solutions of the phosphides M_2P , $\text{M} = \text{Cr}, \text{Mn}, \text{Fe}, \text{Co}$, and Ni , *J. Appl. Phys.* 40 (1969) 1250–1257.
- [23] H. Fujii, T. Hōkabe, T. Kamigaichi, T. Okamoto, Magnetic properties of Fe_2P single crystal, *J. Phys. Soc. Jpn.* 43 (1977) 41–46.
- [24] L. Lundgren, G. Tarmohamed, O. Beckman, B. Carlsson, S. Rundqvist, First order magnetic phase transition in Fe_2P , *Phys. Scr.* 17 (1978) 39–48.
- [25] H. Yibole, F. Guillou, Y.K. Huang, G.R. Blake, A.J.E. Lefering, N.H. Dijk, E. Brück, First-order ferromagnetic transition in single-crystalline $(\text{Mn},\text{Fe})_2(\text{P},\text{Si})$, *Appl. Phys. Lett.* 107 (2015) 162403.
- [26] Z.R. Zhao, T. Jing, G.F. Wang, B.Y. Yang, X.F. Zhang, Influences of sintering temperature on the microstructure and magnetocaloric effect of $\text{Mn}_{1.15}\text{Fe}_{0.85}\text{P}_{0.65}\text{Si}_{0.13}\text{Ge}_{0.2}\text{B}_{0.02}$ prepared by spark plasma sintering, in: *Proceedings of the 2018 IEEE International Magnetics Conference (INTERMAG)*, 2018, pp. 1–5.
- [27] L. Caron, Z.Q. Ou, T.T. Nguyen, D.T. Cam Thanh, O. Tegus, E. Brück, On the determination of the magnetic entropy change in materials with first-order transitions, *J. Magn. Magn. Mater.* 321 (2009) 3559–3566.
- [28] O. Tegus, K. Koyama, J.L. Her, K. Watanabe, E. Brück, K.H.J. Buschow, F.R. de Boer, X-ray diffraction on $\text{MnFeP}_{0.46}\text{As}_{0.54}$ in a magnetic field, *Phys. B: Condens. Matter* 392 (2007) 151–153.
- [29] H. Yabuta, K. Umeo, T. Takabatake, K. Koyama, K. Watanabe, Temperature- and field-induced first-order ferromagnetic transitions in $\text{MnFe}(\text{P}_{1-x}\text{Ge}_x)$, *J. Phys. Soc. Jpn.* 75 (2006) 113707.
- [30] Z.Q. Ou, L. Zhang, N.H. Dung, L. Caron, E. Brück, Structure, magnetism and magnetocalorics of Fe-rich $(\text{Mn},\text{Fe})_{1.95}\text{P}_{1-x}\text{Si}_x$ melt-spun ribbons, *J. Alloy. Compd.* 710 (2017) 446–451.
- [31] B.-G. Kim, Y.-S. Hor, S.-W. Cheong, Chemical-pressure tailoring of low-field, room-temperature magnetoresistance in $(\text{Ca},\text{Sr},\text{Ba})\text{Fe}_{0.5}\text{Mn}_{0.5}\text{O}_3$, *Appl. Phys. Lett.* 79 (2001) 388–390.
- [32] J. Sánchez-Benítez, J.A. Alonso, M.J. Martínez-Lope, A. de Andrés, M.T. Fernández-Díaz, Enhancement of the Curie temperature along the perovskite series $\text{RCu}_3\text{Mn}_4\text{O}_{12}$ driven by chemical pressure of R^{3+} cations ($\text{R} = \text{Rare Earths}$), *Inorg. Chem.* 49 (2010) 5679–5685.